

Integration of EEG source imaging and fMRI during continuous viewing of natural movies[☆]

Kevin Whittingstall^{a,*}, Andreas Bartels^{a,b}, Vanessa Singh^a,
Soyoung Kwon^a, Nikos K. Logothetis^{a,c}

^aMax Planck Institute for Biological Cybernetics, Spemannstrasse 38, D-72076 Tübingen, Germany

^bCentre for Integrative Neuroscience, University of Tübingen, Paul-Ehrlich-Str. 15-17, D-72076 Tübingen, Germany

^cDivision of Imaging Science and Biomedical Engineering, University of Manchester, Manchester M13 9PT, United Kingdom

Received 11 October 2009; revised 19 March 2010; accepted 26 March 2010

Abstract

Electroencephalography (EEG) and functional magnetic resonance imaging (fMRI) are noninvasive neuroimaging tools which can be used to measure brain activity with excellent temporal and spatial resolution, respectively. By combining the neural and hemodynamic recordings from these modalities, we can gain better insight into how and where the brain processes complex stimuli, which may be especially useful in patients with different neural diseases. However, due to their vastly different spatial and temporal resolutions, the integration of EEG and fMRI recordings is not always straightforward. One fundamental obstacle has been that paradigms used for EEG experiments usually rely on event-related paradigms, while fMRI is not limited in this regard. Therefore, here we ask whether one can reliably localize stimulus-driven EEG activity using the continuously varying feature intensities occurring in natural movie stimuli presented over relatively long periods of time. Specifically, we asked whether stimulus-driven aspects in the EEG signal would be co-localized with the corresponding stimulus-driven BOLD signal during free viewing of a movie. Secondly, we wanted to integrate the EEG signal directly with the BOLD signal, by estimating the underlying impulse response function (IRF) that relates the BOLD signal to the underlying current density in the primary visual area (V1). We made sequential fMRI and 64-channel EEG recordings in seven subjects who passively watched 2-min-long segments of a *James Bond* movie. To analyze EEG data in this natural setting, we developed a method based on independent component analysis (ICA) to reject EEG artifacts due to blinks, subject movement, etc., in a way unbiased by human judgment. We then calculated the EEG source strength of this artifact-free data at each time point of the movie within the entire brain volume using low-resolution electromagnetic tomography (LORETA). This provided for every voxel in the brain (i.e., in 3D space) an estimate of the current density at every time point. We then carried out a correlation between the time series of visual contrast changes in the movie with that of EEG voxels. We found the most significant correlations in visual area V1, just as seen in previous fMRI studies (Bartels A, Zeki, S, Logothetis NK. Natural vision reveals regional specialization to local motion and to contrast-invariant, global flow in the human brain. *Cereb Cortex* 2008;18(3):705–717), but on the time scale of milliseconds rather than of seconds. To obtain an estimate of how the EEG signal relates to the BOLD signal, we calculated the IRF between the BOLD signal and the estimated current density in area V1. We found that this IRF was very similar to that observed using combined intracortical recordings and fMRI experiments in nonhuman primates. Taken together, these findings open a new approach to noninvasive mapping of the brain. It allows, firstly, the localization of feature-selective brain areas during natural viewing conditions with the temporal resolution of EEG. Secondly, it provides a tool to assess EEG/BOLD transfer functions during processing of more natural stimuli. This is especially useful in combined EEG/fMRI experiments, where one can now potentially study neural-hemodynamic relationships across the whole brain volume in a noninvasive manner.

© 2010 Elsevier Inc. All rights reserved.

Keywords: EEG; fMRI; Source localization; Natural scenes

1. Introduction

The development of electroencephalography (EEG) and functional magnetic resonance imaging (fMRI) has enabled researchers to study brain function with high temporal and

[☆] This work was supported by the Max Planck Society.

* Corresponding author. Spemannstrasse 38, D-72076 Tübingen, Germany. Tel.: +49 7071 601 1606; fax: +49 7071 601 652.

E-mail address: kevin.whittingstall@tuebingen.mpg.de (K. Whittingstall).

spatial resolution, respectively. These methodologies are especially important given that they are noninvasive and can provide the observation of brain activity across the entire brain volume, something that is often not feasible with invasive recordings. Several studies have provided clear evidence that the signals measured using fMRI are more strongly coupled to the postsynaptic activity (as measured with the local field potential or LFP) than to the population firing rates of cortical neurons [1–4]. Given that the surface EEG is also closely related to the LFP [5], this suggests that combined EEG/fMRI experiments may be useful for noninvasively assessing how cortically generated electric and hemodynamic phenomena are related to each other (so-called neurovascular coupling). However, this integration requires knowledge of the spatial position of the underlying neural activity leading to the scalp-recorded EEG signal. For example, by solving the EEG inverse problem, one can compare the source location of a particular event-related potential (ERP) component with that of a peak BOLD activation site. Correspondence between ERP sources and fMRI activation has been reported in auditory [6–8], visual [9–11] and somatosensory [12] cortex. However, there also exist a growing number of studies which have reported varying degrees of ERP–fMRI correspondence depending on the chosen ERP component [13,14], anatomical area [15] and individual subject [15,16]. There are several causes which may lead to such discrepancy. Firstly, different ERP components within a sensory response most likely reflect diverse neural mechanisms and functions [17] and the neural processes involved in eliciting a particular ERP component may not necessarily translate to an increase in BOLD activation. Therefore, choosing which ERP component to compare to the fMRI data may be difficult. Secondly, ERP studies often rely on brief stimulus events which are based on relatively artificial stimulus settings which may not necessarily involve the same pathways involved in processing during ecologically more relevant settings. For example, recent fMRI evidence suggests that natural stimuli lead not only to very specific activation patterns, but also to more specific inter-regional functional connectivity [18,19]. Given the above, it may be more advantageous to investigate the relationship between the entire ERP source waveform and the fMRI signal from the same cortical area under natural stimulus conditions. However, such comparison is only possible if the ERP signal is on similar time scales as the fMRI signal (~10–20 s) which is challenging given that EEG recordings acquired over relatively long recording periods are often contaminated with various artifacts (noise, eye blinks, eye wanderings, etc.).

Therefore, we wanted to go beyond and ask whether (1) reliable EEG signals could be acquired over long periods of naturalistic stimulation, (2) EEG responses to simple visual features can be reliably localized in these more natural conditions and whether (3) the corresponding sources in primary visual cortex are related to the fMRI signal in the same manner as that obtained using invasive recordings in

nonhuman primates. We addressed these questions by exposing human observers to conditions that resemble those we encounter in real life, by allowing them to freely view a *James Bond* movie, where the brain has to process many features simultaneously and at a rapid rate, with the intensity of the features varying over time. Using an independent component analysis (ICA)-based method, we first removed artifacts in the EEG and then estimated the current density of sources across the entire brain volume. The results show that only voxels within the visual cortex were significantly correlated to the ongoing changes in movie contrast. Additionally, the latency differences between the activity profile of sources in Areas 17, 18 and 19 were comparable to those values obtained from invasive recordings in humans. Lastly, we show that the impulse response function (IRF), which relates the EEG sources to the fMRI signal, was strikingly similar to that obtained from invasive recordings in nonhuman primates. Overall, the results show that this approach for combining EEG and fMRI data is a reliable method that can be used for better understanding the relationship between EEG and fMRI in a noninvasive manner.

2. Methods

2.1. Experimental paradigm

Seven subjects (three females; average age 26 years) with normal or corrected-to-normal vision participated in the study. None of the subjects had any history of neurological or psychiatric illness, and all experimental procedures were approved by the joint ethics committee of the Max Planck Institute and University Hospital, Tübingen, Germany. All seven subjects watched sections of the commercially available movie *James Bond 007—Tomorrow Never Dies* (UK, 1997). Four subjects saw the first 2 min of the movie. In order to test the reproducibility of results not only across different subjects but also across different stimuli, an additional three subjects watched a different 2-min part of the same movie that was chosen to be approximately matched to the first clip in terms of the motion, action and color contrast. All seven subjects were presented with trials that consisted of a 120 s-long movie scene followed by a rest period (a blank screen of 30 s). Note that only data during movie presentation were analyzed, and not the resting data following it, as the aim here was to relate ongoing brain activity with ongoing features of the movie.

The EEG experiment consisted of 25 repetitions (trials) of the same movie clip. In the fMRI experiment, a total of 16 trials were presented, in four sessions with four trials each. In order to reduce eye movements that can cause major artifacts in EEG recordings, subjects were instructed to fixate a central fixation dot present during movie and rest periods. Only during the movie did the fixation dot randomly change color from yellow to green and the subjects' task was to mentally count the number of times the color changed. This

task ensured that the subjects fixated properly throughout the movie. In the EEG experiments, the responses were reported verbally at the end of each trial (during the 30 s pause between trials), and in the fMRI experiments subjects reported verbally at the end of each scanning session (i.e., after four movie trials). The verbal mode of responding after data collection helped us to avoid confounds that would have arisen with concurrent motor responses.

2.2. EEG Acquisition and data preprocessing

Continuous 64-channel EEG was acquired at a sampling rate of 500 Hz (Vision Recorder, Brain Product, Inc., Munich, Germany). The electrode placement followed the international 10–20 system, with a reference electrode at the FCz. Two electrodes were placed under and on the outer canthus of the right eye to record the electro-oculogram (EOG). Offline data pre-processing was done using Vision-Analyser (Brain Products). The data were bandpassed between 0.5 and 45 Hz and epoched based on marker position (i.e., stimulus onset). These preprocessed data were then converted into a format compatible with the EEGLab software [20] for further analyses.

2.3. EEG Artifact correction

Given the specific design of our experiment characterized by the 2-min-long movie stimulus, EEG artifacts (especially eye blinks) posed a serious problem for data interpretation and analysis (Fig. 1). To avoid interference from ocular artifacts, a common strategy used in traditional EEG studies using brief trials is to reject all EEG trials containing artifacts larger than a predetermined EEG voltage value. However, when data are limited, when blinks and eye movements occur too frequently or, as in our case, when trials last very long, the amount of data lost to the artifact rejection may be unacceptable. In this scenario, it is therefore more advantageous to correct for artifacts while retaining all trials for subsequent analysis. Previous studies have used correction techniques based on linear regression [21] and ICA [22]. ICA attempts to separate EEG processes whose time waveforms are maximally independent of each other, and several laboratories have successfully demonstrated that ICA can separate multichannel EEG recordings into meaningful and nonmeaningful processes (such as eye blinks and lateral eye movement [22,23]). However, deciding and rejecting the independent components that represent artifacts are nontrivial issues. One approach relies on visual inspection, which may result in some artifacts going unrecognized. Another may rely on objective criteria, such as removing independent components (ICs) based on the basis of their variance, kurtosis or particular combinations thereof. Here we used an automated and objective approach that limited the level of manual subjective intervention and that performed very well for our purposes. Our approach is described below.

We defined the following criteria according to which ICs would be automatically classified as artifacts and subsequently removed from the data.

The first rejection criteria exploited the temporal waveforms of the ICs. We first rectified all IC time courses (64 per subject in our case) and converted the amplitude values of each of them to z -scores. We then set a threshold of seven and rejected all ICs whose temporal activation at any point in time exceeded this threshold. This threshold was chosen based on visual inspection of the data and is consistent with values obtained in another recent EEG study [24]. In other words, this threshold identified all rarely occurring, high-amplitude events. Alone, this approach worked very well for removing transient, large-amplitude artifacts such as blinking. However, this approach could not successfully remove muscle-originated artifacts, which often show up as low-amplitude, high-frequency activity which is concentrated around the temporal electrodes. For this, we designed a second rejection criterion, based on the spatial maps of the remaining ICs. IC spatial maps represent the relative contribution of each electrode to that particular IC. We converted the IC weight value at each electrode to a z -score and excluded a spatial map if the z -score at any electrode exceeded a value of 9, or if the combination of any two electrodes exceeded a value of 15. This approach eliminated spatial maps consisting of a few electrodes whose activity was abnormally high relative to the mean activity across electrodes. In other words, this criterion was designed in order to identify spatial maps whose activity was focal and concentrated across a few channels, which is different than the otherwise smooth IC maps expected from true brain activity. An example of this artifact-correction routine is shown in Fig. 2, which shows three exemplar ICs from one subject. The temporal activation of IC no. 3 is highly correlated with the signal measure in the EOG electrode, indicating that this component represents blinking. Its corresponding spatial map corroborates this: the activity here is clearly concentrated around frontal electrodes, which again is symptomatic of blinking [25]. IC no. 47 does not contain such blinking artifacts, but clear high-frequency bursts are evident. The corresponding spatial map shows clustered activity around the right temporal electrodes, which for the most part reflects muscular artifacts [26]. The last component (IC no. 8) on the other hand does not contain such transient spikes in its temporal activation nor is its spatial topography concentrated around a few electrodes. Rather, its spatial map is smooth with a dipolar pattern, indicating that this component reflects ‘true’ neural activity. In this particular example, IC no. 3 and IC no. 47 would be rejected while component IC no. 8 is retained. For each subject, all components not adhering to the aforementioned criteria were removed and the remaining, artifact-free ICs were back-projected to construct a new EEG data set, which was downsampled to 200 Hz and then averaged across trials for further analysis.

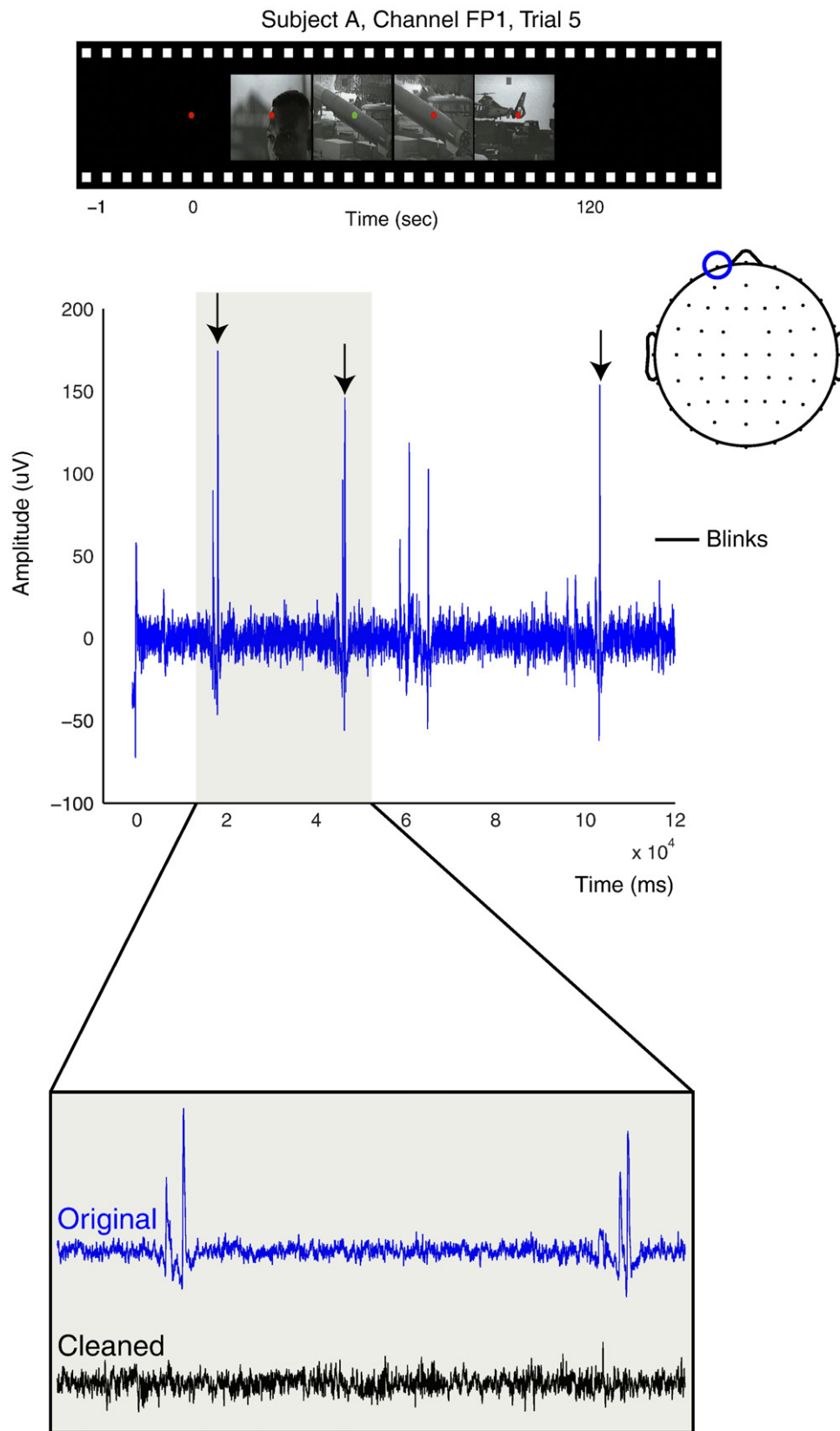


Fig. 1. An example of the EEG signal (electrode F1) recorded from one subject during continuous viewing of a 2-min-long natural movie clip. The high amplitude transients represent blinks, which when removed result in a cleaner EEG signal that can then be used for further analysis (details of the artifact rejection technique can be found in the Methods section).

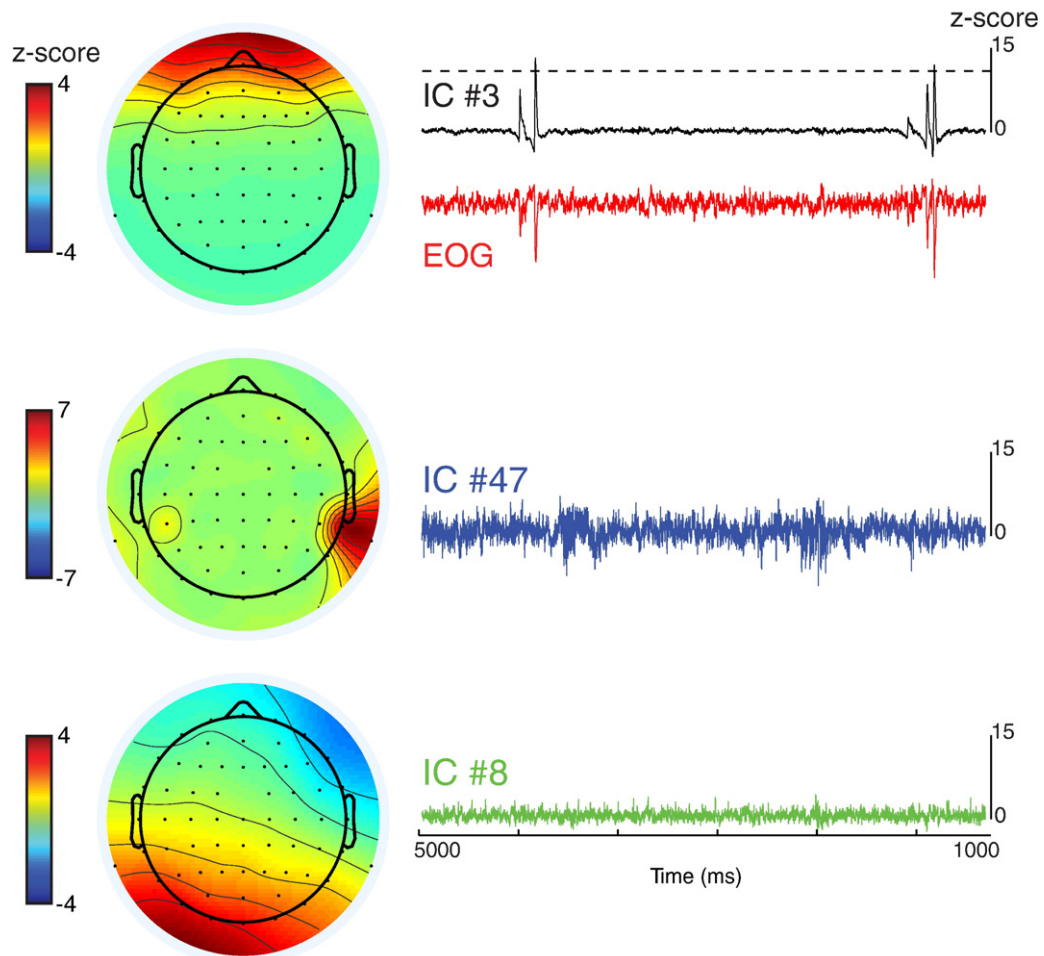


Fig. 2. Three ICA components from the EEG data shown in Fig. 1. The time course of IC no. 3 contains large transients that correspond to blinks. This is confirmed by its resemblance to the EOG signal and its scalp topography that shows a strong, far-frontal projection that is typical of eye artifacts. IC no. 47 does not contain large amplitude transients as in IC no. 3, but strong bursts in high-frequency activity, coupled with a focal activation around the right temporal electrodes, indicate muscle movement or twitching, which again is typical for such artifacts. The last component (IC no. 8) does not consist of any of the artifacts mentioned above, and its scalp map is relatively smooth across electrodes with a dipolar-like distribution. In this example, IC no. 3 and IC no. 47 are removed from the data and IC no. 8 (along with remaining similar components) is retained for further analysis. Details of the threshold used for identifying artifactual components can be found in the Methods section.

In the end, our artifact-correction approach allowed us to remove all artifactual components of the EEG signal while retaining all trials.

2.4. EEG Source imaging

The first goal of this study was to show whether EEG source imaging could give stable and reliable results during relatively long EEG recording periods. Therefore, the first step was to transform the EEG data from ‘scalp space’ into ‘source space.’ This was done using low-resolution electromagnetic tomography (LORETA) [27,28]. LORETA falls into the class of distributed source models that do not require a priori knowledge regarding the number of active sources and thus are advantageous for the localization of poorly known activity distributions. LORETA is capable of correct, although blurred (low-resolution), 3D localization as has

been demonstrated in simulation work as well as in empirical validations [28–30]. The source space was calculated with the boundary element method applied to the standardized Montreal Neurological Institute (MNI) brain volume (MNI152) consisting of 6239 cortical gray matter voxels at 5-mm resolution. LORETA source maps reflect the current density of a source in a particular voxel at a particular time point. That is, each of the 6239 voxels consisted of a 2-min-long time series representing how the strength of that particular source varies during the presentation of the movie. Given the relatively low resolution of the LORETA imaging method, the activity in a single voxel is representative of the activity within the nearby-surrounding volume. With this in mind, we defined 455 regions of interest (ROIs) that were based on seed points equally distributed throughout the brain such that each Brodmann area was sampled equally with respect to its volume represented in the source space. All

voxels that fell within a 10-mm radius of the seed point were averaged together, resulting in 455 ROIs, each with time courses representing the modulations of the source strength within that particular ROI.

2.5. fMRI Acquisition and analysis

Whole-brain images (33 slices; 2.6 mm thick, 0.4 mm gap, 64×64 pixels in-plane resolution, overall resolution 3×3×3 mm) were collected on a 3-T TIM Siemens scanner using an echo-planar imaging sequence. Scans were acquired with a repetition time of 2.3 s and echo time of 40 ms. Additionally, a T1-weighted structural scan was acquired for each subject (1 mm isotropic resolution). SPM5 was used to spatially realign the images to reduce movement artifacts, and slices were realigned temporally to compensate for acquisition time lags. Images were spatially normalized to the MNI template and spatially smoothed using a Gaussian kernel of 6 mm full-width at half height. We then high-pass filtered the BOLD signal with a cut-off of 256 s and then averaged the signal over the 16 stimulus presentations. Spherical ROIs (radius=10 mm) were placed at the same seed points used in the EEG source imaging analysis, and the mean BOLD signal from each ROI was extracted using the marsbar toolbox (<http://marsbar.sourceforge.net>).

2.6. Movie features

We extracted the low-level visual content of the movie clips in terms of the pixel-wise luminance changes (or temporal contrast), as this was shown previously to correlate well with activity in early visual cortex [31]. In short, this was done as follows. Visual contrast changes were calculated as follows: each pixel of each movie frame was converted to luminance, and the difference between each sequential pair of movie frames was calculated. Our measure of temporal contrast was the mean of the absolute values of each of these luminance-difference frames. For the fMRI analysis, the time series of temporal contrast was convolved using the canonical hemodynamic response function provided in SPM5, prior to using it as a regressor.

2.7. Estimated impulse response function

Using the EEG source waveform and corresponding BOLD signal in area V1, we calculated the IRF between the two using a prewhitening-based correlation analysis. For this, the input (current density) data was first prewhitened by fitting it to a 10th-order autoregressive model. The parameters of the autoregressive model were estimated by using the least-square method (i.e., by minimizing the standard sum of squares, forward prediction errors). Correlation analysis was applied after subjecting the output (BOLD) data to the same filter. This operation was carried out using the (spatial) mean neural and hemodynamic signals within area V1 for each subject. In each subject, the calculated IRF was normalized to its peak and then averaged over all subjects.

3. Results

In the present study, we aimed to integrate EEG and fMRI signals recorded in an ecologically meaningful setting in which subjects viewed 2-min-long action movie clips. This required as a first step the development of robust and efficient artifact-removal strategies for the EEG data, which are presented in the Methods section. The second aim was twofold: first, we wanted to spatially localize EEG signals that were related to the continuously varying feature of visual contrast change throughout the movie clip. To achieve this, we first used LORETA to estimate the current density for every voxel in the brain for every time point. This yielded a time course for every voxel from which we then computed the correlation coefficient between it and the visual feature-intensity timeline. Second, we wanted to infer the transfer function between EEG current density of the localized region to the fMRI signal of the same region.

We found that over all subjects, the mean correlation between EEG source strength and movie contrast was highest within the calcarine sulcus of the visual cortex (mean \pm S.D., 0.27 ± 0.01 , $P < .01$; Fig. 3A) and quickly decreased when moving to higher visual areas. Note that these findings were highly robust, also in light of altered analysis parameters. For example, the EEG source localization map was very similar to the one shown here when scene cuts were regressed out from the EEG data and from the visual feature timeline in the analysis. Cross-correlation analysis revealed that the correlation was highest when the EEG source waveform was shifted 109 ± 0.03 ms in Area 17, 115 ± 0.05 ms in Area 18 and 117 ± 0.07 ms in Area 19 (Fig. 3B). Since the visual contrast changes also correlated best with BOLD signal in V1 (not shown, but see equivalent results in Fig. 4c, f in Ref. [32]), this co-localization of EEG source imaging and BOLD signal strongly justified the calculation of the underlying transfer function (IRF) between the two signals. Fig. 3C shows the resulting mean estimated IRF over all seven subjects. Here, the peak occurred at 5.26 ± 0.88 s. In other words, increases in the V1 BOLD signal occur approximately 5 s after the changes in V1 EEG activity.

4. Discussion

In this study, we asked whether (1) reliable EEG signals could be acquired over long periods of naturalistic stimulation, (2) EEG responses to simple visual features can be reliably localized in these more natural conditions and whether (3) the corresponding sources in primary visual cortex are related to the fMRI signal in the same manner as that obtained using invasive recordings in nonhuman primates.

Firstly, our results show that the estimated current density in the primary visual cortex (Area 17) was strongly correlated to changes in movie contrast. This is consistent with previous experiments using single-cell recordings [33],

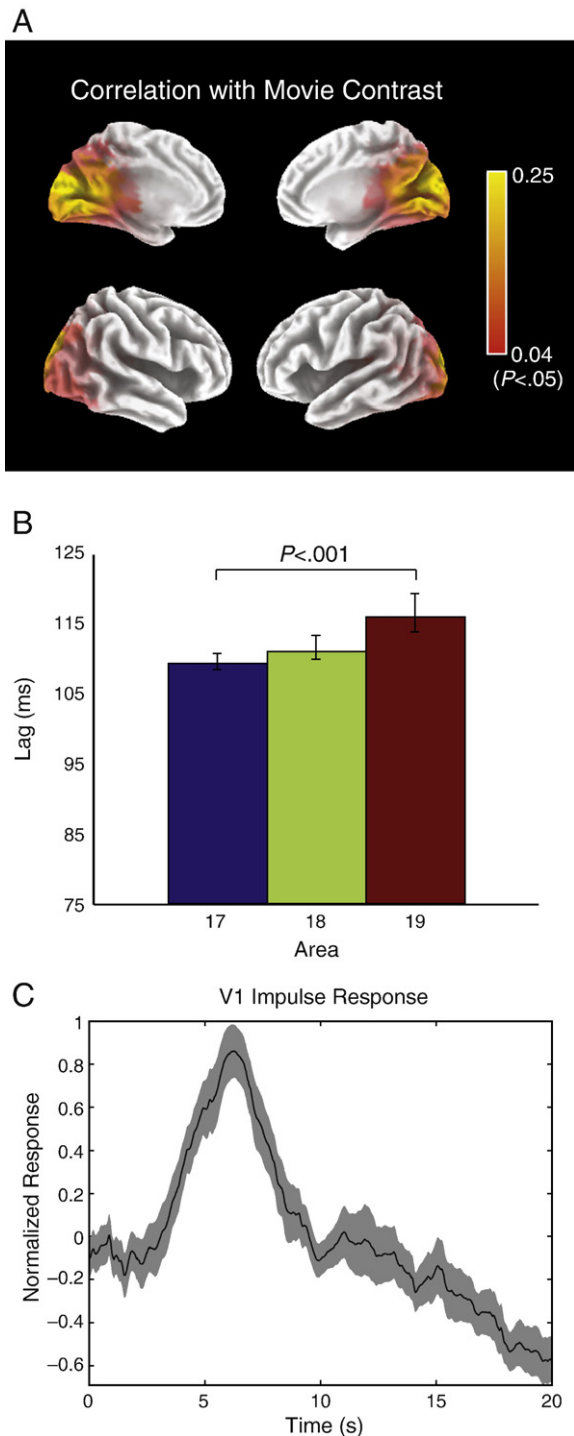


Fig. 3. EEG source imaging: (A) Whole-brain correlation of EEG source signals with visual contrast changes in the movie stimulus reveals a primary involvement of early visual areas, in particular area V1 (displayed as a mean over seven subjects). (B) With cross-correlations, the best correlation between neural activity in Area 17 and movie contrast was observed at time lag which tended to be earlier than that in Area 18 and 19 (results represent the mean over seven subjects; error bars: S.E.M.). (C) The IRF which relates the estimated current density (input) to the BOLD signal (output) in Area 17. The black line represents the mean over all subjects and the shade represents the S.E.M.

fMRI [31] and optical imaging [34]. Significant (albeit weaker) correlations were also found in Areas 18 and 19 and failed to reach statistical significance in higher cortical areas. Secondly, it is interesting to note that despite the fact that contrast changes in the movie were related to recognizable scenes and objects, the prime location affected by these changes resided in V1, indicating an increasing contrast invariance in higher-level areas [31,35]. Thirdly, cross-correlation analysis revealed that the mean response latency in Area 17 was slightly earlier than that observed in Area 18 and significantly earlier than responses in Area 19 ($P < .01$). This trend is consistent with a recent study where visual stimuli were presented to subjects (selected for clinical purposes) with subdural electrodes implanted over different regions of the visual cortex [36], as well as with signal arrival times recorded across distinct visual regions in nonhuman primates [37]. Taken together, these EEG source imaging results indicate that the artifact-correction methodology correctly identified and removed unwanted nonneural components of the EEG signal while preserving those containing information which reflected the movie stimulus. While these three relatively straightforward criteria seemed to reliably remove the strongest artifactual components, further study is needed for delineating more subtle artifacts from true neural activity [38].

Finally, we investigated how the estimated current density within the visual cortex was related to the BOLD signal from the same area. Here, we found that the IRF relating the two signals was very similar to the IRF obtained from simultaneous intracortical electrophysiology and BOLD signal measurements in primary visual cortex of nonhuman primates [1]. This provides evidence that, at the very least, certain properties of the estimated EEG source strength are similar to the LFP obtained when using invasive neurophysiological recording techniques.

Overall, our results demonstrate that functional EEG mapping can be achieved over relatively long stimulus periods allowing the mapping of ongoing feature variations. This suggests that more complex stimuli presented in more realistic conditions can be used for EEG experiments in order to simultaneously study the dynamics of neural signals within the entire brain volume. This approach thus opens up a whole range of paradigms hitherto reserved to fMRI, with the additional benefit that the EEG source imaging signals have a superior temporal scale which allows for better identification of neural processes that are too fast to be reliably detected by the slower BOLD signal. Taken together, our approach lends itself to studying EEG/fMRI signal correlations over long recording periods, thus providing a new tool for noninvasive investigations of the human brain.

Acknowledgment

Special thanks to Yusuke Murayama for helpful suggestions and to Dorothy Bishop for helpful advice regarding the ICA artifact-correction routine.

References

- [1] Logothetis NK, et al. Neurophysiological investigation of the basis of the fMRI signal. *Nature* 2001;412(6843):150–7.
- [2] Viswanathan A, Freeman RD. Neurometabolic coupling in cerebral cortex reflects synaptic more than spiking activity. *Nat Neurosci* 2007; 10(10):1308–12.
- [3] Rauch A, Rainer G, Logothetis NK. The effect of a serotonin-induced dissociation between spiking and perisynaptic activity on BOLD functional MRI. *Proc Natl Acad Sci U S A* 2008;105(18):6759–64.
- [4] Goense JB, Logothetis NK. Neurophysiology of the BOLD fMRI signal in awake monkeys. *Curr Biol* 2008;18(9):631–40.
- [5] Whittingstall K, Logothetis NK. Frequency-band coupling in surface EEG reflects spiking activity in monkey visual cortex. *Neuron* 2009;64 (2):281–9.
- [6] Menon V, et al. Combined event-related fMRI and EEG evidence for temporal-parietal cortex activation during target detection. *NeuroReport* 1997;8(14):3029–37.
- [7] Mulert C, et al. Integration of fMRI and simultaneous EEG: towards a comprehensive understanding of localization and time-course of brain activity in target detection. *Neuroimage* 2004;22(1):83–94.
- [8] Opitz B, et al. Combining electrophysiological and hemodynamic measures of the auditory oddball. *Psychophysiology* 1999;36(1): 142–7.
- [9] Di Russo F, et al. Identification of the neural sources of the pattern-reversal VEP. *Neuroimage* 2005;24(3):874–86.
- [10] Kruggel F, et al. Recording of the event-related potentials during functional MRI at 3.0 Tesla field strength. *Magn Reson Med* 2000;44 (2):277–82.
- [11] Vanni S, et al. Sequence of pattern onset responses in the human visual areas: an fMRI constrained VEP source analysis. *Neuroimage* 2004;21 (3):801–17.
- [12] Grimm C, et al. A comparison between electric source localisation and fMRI during somatosensory stimulation. *Electroencephalogr Clin Neurophysiol* 1998;106(1):22–9.
- [13] Whittingstall K, Stroink G, Schmidt M. Evaluating the spatial relationship of event-related potential and functional MRI sources in the primary visual cortex. *Hum Brain Mapp* 2006;28(2):134–42.
- [14] Whittingstall K, et al. Correspondence of visual evoked potentials with fMRI signals in human visual cortex. *Brain Topogr* 2008;21(2): 86–92.
- [15] Liljestrom M, et al. Comparing MEG and fMRI views to naming actions and objects. *Hum Brain Mapp* 2009;30(6):1845–56.
- [16] Vitacco D, et al. Correspondence of event-related potential tomography and functional magnetic resonance imaging during language processing. *Hum Brain Mapp* 2002;17(1):4–12.
- [17] Shigeto H, et al. Visual evoked cortical magnetic responses to checkerboard pattern reversal stimulation: a study on the neural generators of N75, P100 and N145. *J Neurol Sci* 1998;156(2):186–94.
- [18] Bartels A, Zeki S. Functional brain mapping during free viewing of natural scenes. *Hum Brain Mapp* 2004;21(2):75–85.
- [19] Bartels A, Zeki S. Brain dynamics during natural viewing conditions— a new guide for mapping connectivity in vivo. *Neuroimage* 2005;24(2): 339–49.
- [20] Delorme A, Makeig S. EEGLAB: an open source toolbox for analysis of single-trial EEG dynamics including independent component analysis. *J Neurosci Methods* 2004;134(1):9–21.
- [21] Gratton G, Coles MG, Donchin E. A new method for off-line removal of ocular artifact. *Electroencephalogr Clin Neurophysiol* 1983;55(4): 468–84.
- [22] Jung TP, et al. Removing electroencephalographic artifacts by blind source separation. *Psychophysiology* 2000;37(2):163–78.
- [23] Jung TP, et al. Removal of eye activity artifacts from visual event-related potentials in normal and clinical subjects. *Clin Neurophysiol* 2000;111(10):1745–58.
- [24] Ball T, et al. Signal quality of simultaneously recorded invasive and non-invasive EEG. *Neuroimage* 2009;46(3):708–16.
- [25] Joyce CA, Gorodnitsky IF, Kutas M. Automatic removal of eye movement and blink artifacts from EEG data using blind component separation. *Psychophysiology* 2004;41(2):313–25.
- [26] Crespo-Garcia M, Atienza M, Cantero JL. Muscle artifact removal from human sleep EEG by using independent component analysis. *Ann Biomed Eng* 2008;36(3):467–75.
- [27] Pascual-Marqui RD, et al. Functional imaging with low-resolution brain electromagnetic tomography (LORETA): a review. *Methods Find Exp Clin Pharmacol* 2002;24(Suppl C):91–5.
- [28] Pascual-Marqui RD, et al. Low resolution brain electromagnetic tomography (LORETA) functional imaging in acute, neuroleptic-naive, first-episode, productive schizophrenia. *Psychiatry Res* 1999;90 (3):169–79.
- [29] Anderer P, et al. Differential effects of normal aging on sources of standard N1, target N1 and target P300 auditory event-related brain potentials revealed by low resolution electromagnetic tomography (LORETA). *Electroencephalogr Clin Neurophysiol* 1998;108(2): 160–74.
- [30] Worrell GA, et al. Localization of the epileptic focus by low-resolution electromagnetic tomography in patients with a lesion demonstrated by MRI. *Brain Topogr* 2000;12(4):273–82.
- [31] Bartels A, Zeki S, Logothetis NK. Natural vision reveals regional specialization to local motion and to contrast-invariant, global flow in the human brain. *Cereb Cortex* 2008;18(3):705–17.
- [32] Bartels A, Logothetis NK, Moutoussis K. fMRI and its interpretations: an illustration on directional selectivity in area V5/MT. *Trends Neurosci* 2008;31(9):444–53.
- [33] Henrie JA, Shapley R. LFP power spectra in V1 cortex: the graded effect of stimulus contrast. *J Neurophysiol* 2005;94(1):479–90.
- [34] Lu HD, Roe AW. Optical imaging of contrast response in macaque monkey V1 and V2. *Cereb Cortex* 2007;17(11):2675–95.
- [35] Avidan G, et al. Contrast sensitivity in human visual areas and its relationship to object recognition. *J Neurophysiol* 2002;87(6): 3102–16.
- [36] Yoshor D, et al. Receptive fields in human visual cortex mapped with surface electrodes. *Cereb Cortex* 2007;17(10):2293–302.
- [37] Schmolesky MT, et al. Signal timing across the macaque visual system. *J Neurophysiol* 1998;79(6):3272–8.
- [38] Delorme A, Sejnowski T, Makeig S. Enhanced detection of artifacts in EEG data using higher-order statistics and independent component analysis. *Neuroimage* 2007;34(4):1443–9.